Electronic Supplementary Material (ESI) for Physical Chemistry Chemical Physics.
This journal is © the Owner Societies 2015

Supporting information for: A Means to an Interface: Investigating Monoethanolamine Behavior at an Aqueous Surface

Laura E. McWilliams, Nicholas A. Valley, Sumi N. Wren, and Geraldine L. Richmond

E-mail:

DFT method evaluation

VSF spectra for aqueous 10 M MEA solutions were calculated with six combinations of xc–functionals (B3LYP, B2PLYP and MP2) and basis sets (6–311++G(2d,2p) or aug–cc–pVTZ). The calculated spectra were compared to experimental spectra in both *ssp*– and *sps*–polarization, with deviation in peak position and relative intensity of spectral peaks used to determine the best match between calculated and experimental spectra. Supporting Figure 1 shows the six calculated *ssp* spectra offset from the 10 M MEA *ssp* experimental spectra, with the main contributing experimental peaks highlighted with vertical guides. For both the bending and stretching *ssp* spectra, the 6–311++G(2d,2p) basis set performs better than the aug–cc–pVTZ. Additionally, the B2PLYP and MP2 functionals better predict experimental peak positions.

Supporting Figure 2 shows calculated and experimental *sps* spectra in the CH stretching region of the vibrational spectra. Only *sps* spectra of the (a) B2PLYP and (b) MP2 xc–functionals are shown, as they were the closest matches to the experimental *ssp* spectra. However, in *sps*

*To whom correspondence should be addressed

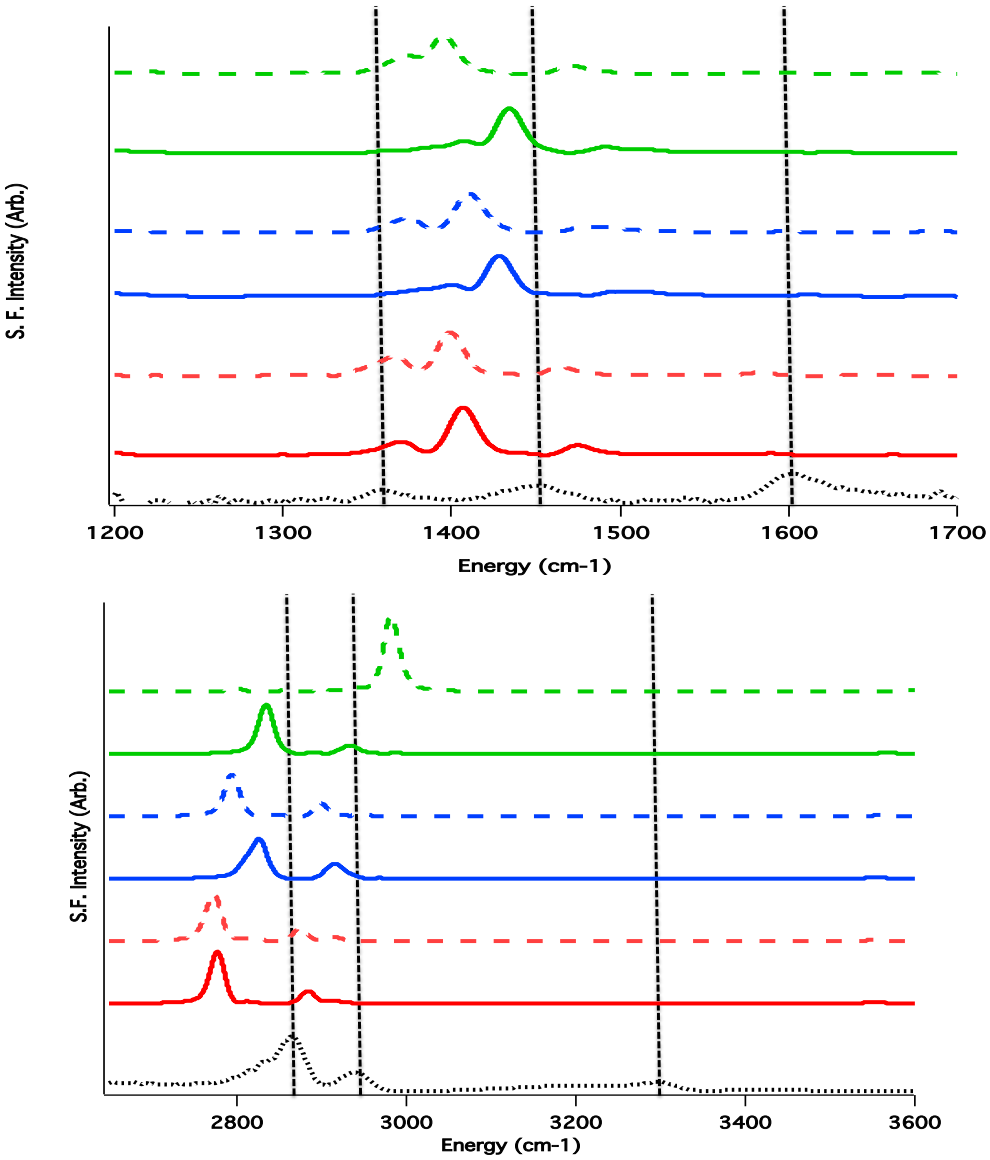

Figure 1: Experimental (dashed black) and calculated (colored) VSF spectra for 10 M MEA solution in *ssp* in the bending region (top) and the stretching region (bottom). Calculations for B3LYP—6311G++(2d,2p) (red solid); B3LYP—aug-ccpVTZ (red dashed); B2PLYP—6311G++(2d,2p) (blue solid); B2PLYP—aug-ccpVTZ (blue dashed); MP2—6311++G(2d,2p) (green solid); and MP2—aug-ccpVTZ (green dashed) are shown. Spectra offset for clarity with guide lines for experimental peaks.

the MP2 functional no longer accurately predicts experimental spectra; rather the B2PLYP is favored. As demonstrated in Supporting Figure 2(a) (along with Figure 4 in the manuscript) , the B2PLYP–6311G++(2d,2p) is the preferred functional–basis set combination for calculating the MEA spectra.

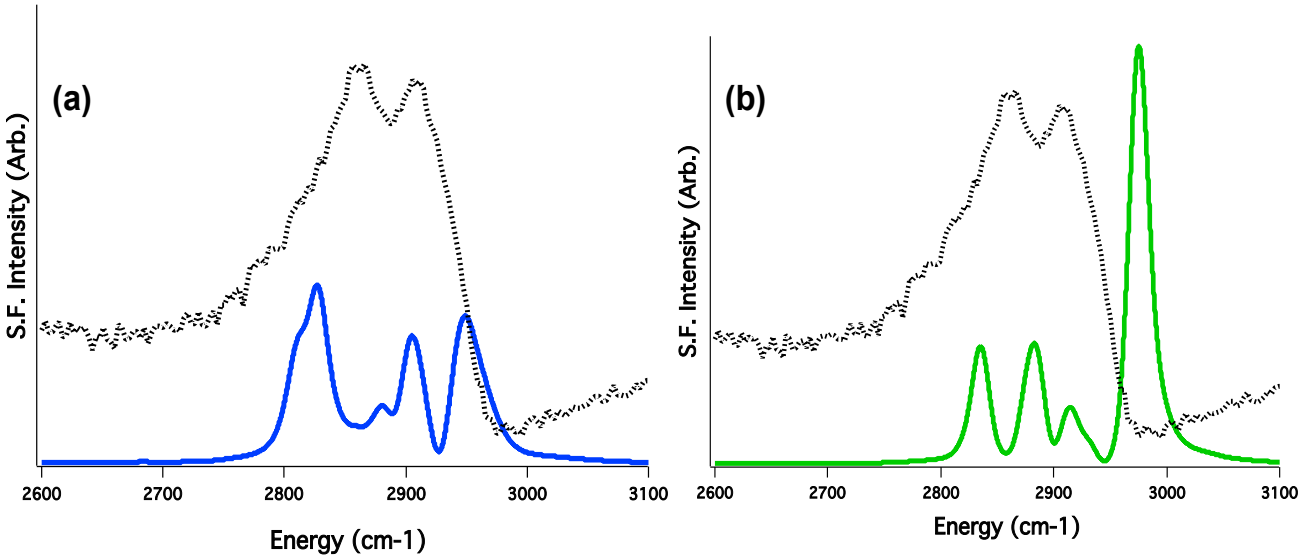

Figure 2: Experimental (dashed black) and calculated (colored) VSF spectra for 10 M MEA solution in *sps* in the CH stretching region. Calculations for (a) B2PLYP—6311G++(2d,2p) (blue solid) and (b) MP2–6311++G(2d,2p) (green solid) shown.

DFT structures

Nine unique MEA gas–phase DFT structures were matched (via dihedral angle binning) with MEA conformers extracted from the MD simulations. The DFT and MD conformers were defined based on 4 unique dihedral angles (D1–D4), as shown in Figure 3, where D1=N–C–C–O; D2=C–C–O–H; D3=C–C–N–H^a; and D4=C–C–N–H^b. The optimized DFT structures' dihedral angles are listed in Table 1 along with the range of dihedrals used to define the MD structures. For the MD structural assignments, the range of angles applies to rotation in both directions.

The MD conformers' dihedral distributions were extracted from the simulations and matched to representative DFT structures. The optimized DFT structures correspond to peaks in the MD

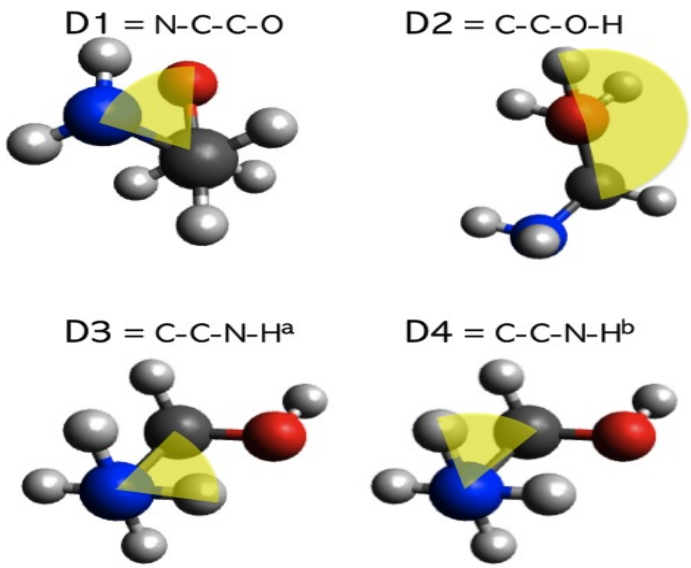

Figure 3: The four dihedrals used to define the DFT and match to the MD conformers. H^a and H^b designate the two different amine hydrogens.

dihedral distributions, as shown in Figure 4, with the exception of the MEA1 conformer whose anti configuration does not correspond to a maximum in the dihedral distribution but was included to fully represent the conformational space. Unsurprisingly, the MD conformer matching showed most MEA molecules adopt gauche conformations ($> 90\%$) while few MEA molecules adopt anti conformations. The largest abundance of MD conformers were assigned to DFT structure MEA14 ($\sim$20%).

Table 1: DFT structures and energies calculated at B3LYP/6-311++G(2d,2p) level of theory. Conformer ranges for MD simulations that matched the DFT structures.

MD Conformer	DFT energy (Hartree)	DFT Dihedral Angle (°)				Dihedral Range (°) for MD Assignments			
		D1	D2	D3	D4	D1	D2	D3	D4
MEA1	-209.094229	-179.5	-68.7	-72.7	168.2	150–180	0–180	0–180	0–180
MEA10	-209.099279	57.9	-43.8	-163.6	77.1	30–90	0–60	150–180	30–90
MEA11	-209.090517	70.5	-172.6	-168.9	72.3	30–90	150–180	150–180	30–90
MEA13	-209.093947	60.3	-76.4	-64.6	56.9	30–90	30–90	30–90	30–90
MEA14	-209.096063	60.0	-177.6	-56.0	61.7	30–90	150–180	30–90	30–90
MEA15	-209.095663	58.2	71.1	-51.3	65.9	30–90	30–90	30–90	30–90
MEA16	-209.095583	63.1	71.9	-55.4	-174.6	30–90	30–90	30–90	150–180
MEA17	-209.096472	54.2	-72.6	-84.5	157.6	30–90	30–90	60–120	130–180
MEA18	-209.096517	64.8	-169.9	-60	-178.2	30–90	150–180	30–90	150–180

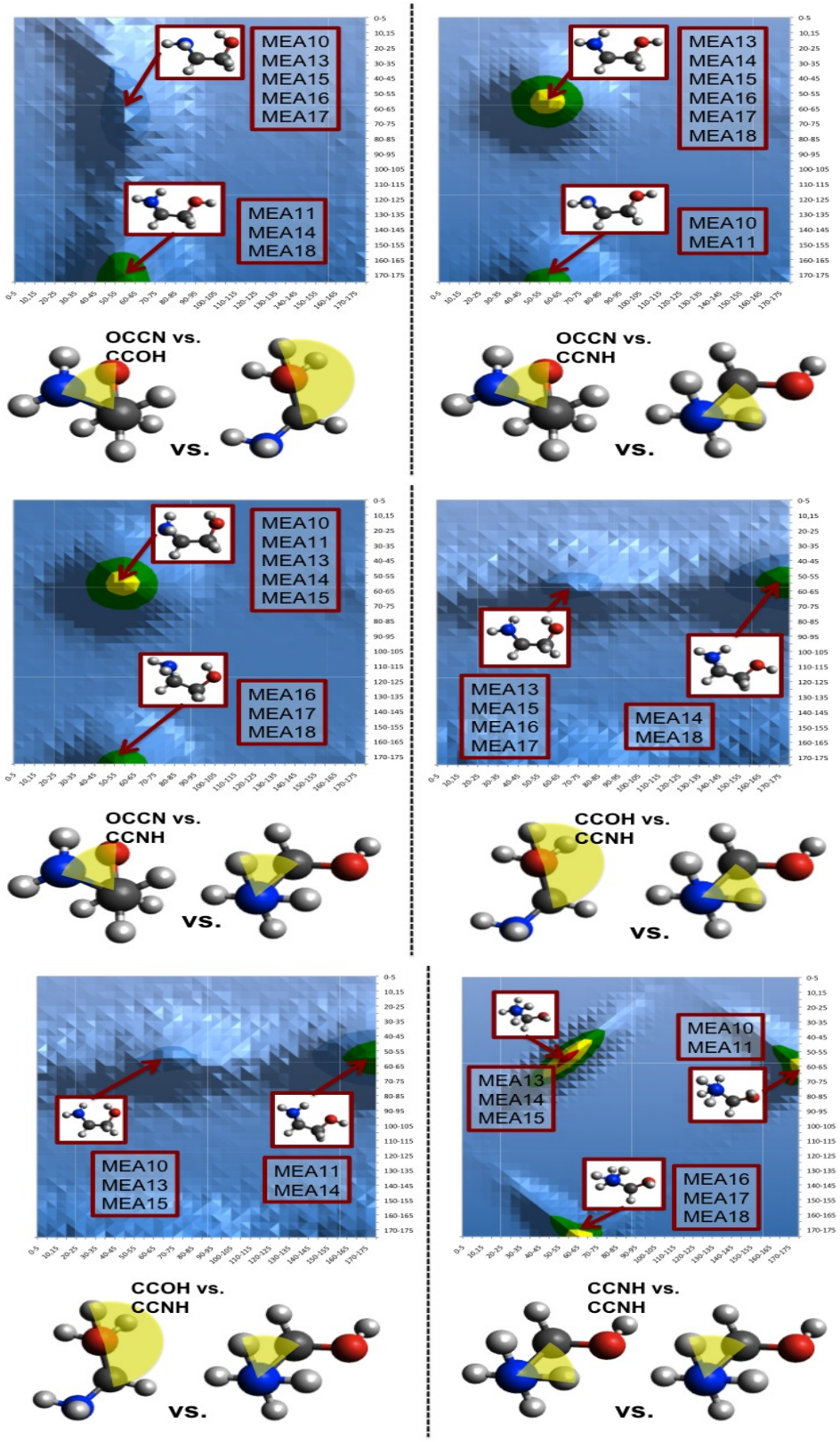

Figure 4: MEA correlated MD dihedral distributions. Maxima are highlighted with representative structural cartoons and labeled with the corresponding DFT structures. Color scheme for z–axis follows that outlined in the manuscript, where cooler colors represent less population and warmer colors represent greater population.

Deuterated *ssp* spectra of 10 M MEA

Spectra in the bending region of the vibrational spectrum were acquired in both H_2O and D_2O to assist in mode assignments. In Supporting Figure 4(a), spectra of the neat H_2O and D_2O interfaces are shown, with the free OH (1625 cm^{-1}) and free OD ($\sim$1210 cm^{-1}) strongly contributing to observed signal. Supporting Figure 4(b) shows 10 M MEA solutions in different aqueous solvents: H_2O for the blue trace and D_2O for the purple trace. Exchange of the amine hydrogens with the solvent results in a loss of the peak at $\sim$1595 cm^{-1} in the D_2O sample; however, retention of the peaks at 1448 cm^{-1} and 1360 cm^{-1} is observed.

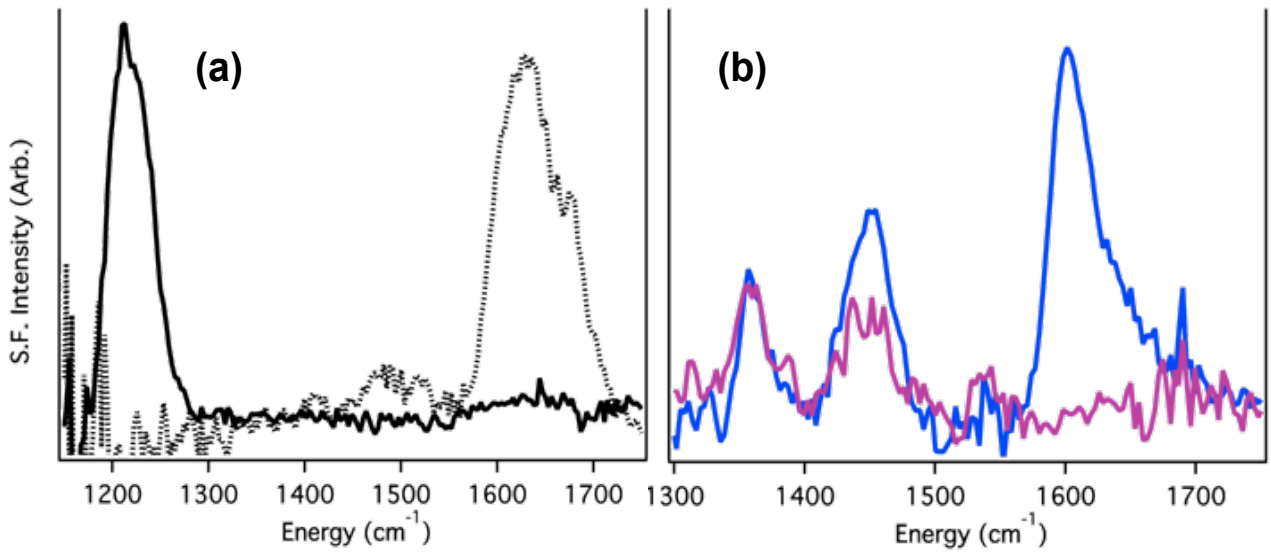

Figure 5: Spectra acquired in bending region of vibrational spectrum in *ssp*–polarization. (a) H_2O (grey dashed) and D_2O (black solid) and (b) 10 M MEA in H_2O (blue) and 10 M MEA in D_2O (purple)

Gibbs adsorption calculations

Surface pressure, π, is plotted as a function of bulk MEA concentration in Supporting Figure 5(a). The Gibbs adsorption equations may be used to relate surface tension (or surface pressure) of a solute with surface excess concentrations, average area per molecule, the relative adsorption or the surface mole fraction of the solute.[1–4] In Equation 1, the maximum surface excess (Γ_i) can be

extracted from the surface pressure by performing a linear fit of the surface pressure values versus the natural log of the bulk activities, as shown in Supporting Figure 5(b).

$$\Gamma_{MEA} = \frac{1}{RT}\left(\frac{\partial \pi}{\partial ln\, a_{MEA}}\right)_{T,P} \tag{1}$$

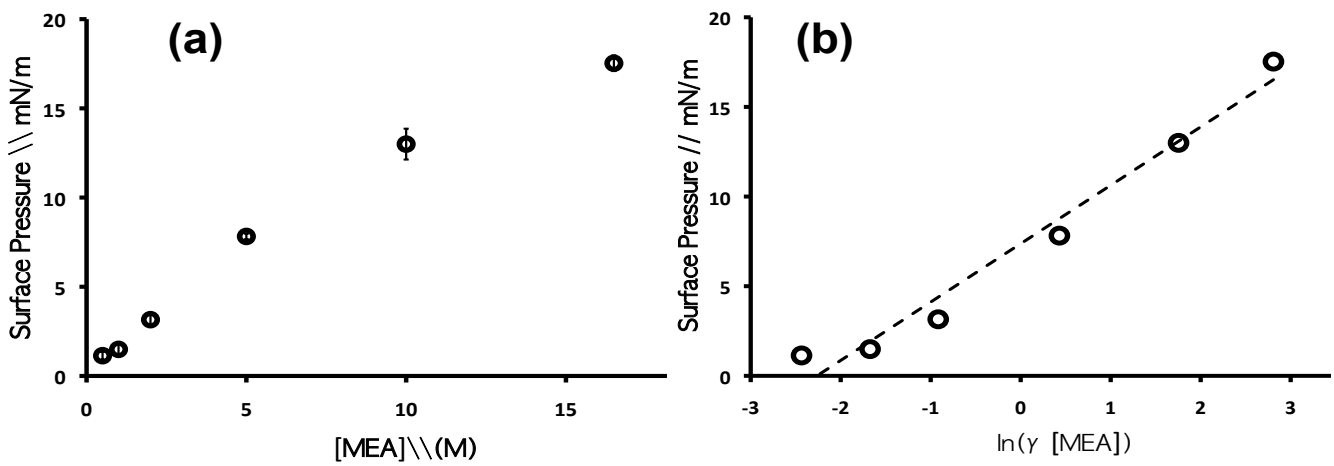

Figure 6: (a) MEA surface pressure (π, mN/m) plotted as a function of bulk MEA concentration. Error bars are one standard deviation from the average of 3–10 data points. (b) MEA surface pressure plotted as a function of natural log of the MEA activities. The dashed line is a fit to the data.

Bulk concentrations of MEA were corrected to activities (α_i) using the activity coefficients (γ_i) derived by Hilliard.[5] The slope of the fit line in Figure 5 (b) was inverted to give the average area per molecule. For MEA, the average area per molecule was found to be $\sim$126 Å^2/molecule.

Additionally, the surface mole fraction may be calculated from the Gibbs equation of relative adsorption ($\Gamma_{2,1}$) as outlined by Tyrode, et al.,[3] via Equation 2.

$$\Gamma_{MEA,H_2O} = -\frac{x\left(\frac{\partial \eta}{\partial x}\right)_{T,P}}{RT\left(1 + x\frac{\partial ln\,\gamma}{\partial x}\right)} = \Gamma_{MEA} - \Gamma_{H_2O}\frac{x}{1-x} \tag{2}$$

where x is the bulk mole fraction of MEA, γ is the activity coefficient from Hilliard, η is the surface tension of MEA, and Γ_{H_2O} and Γ_{MEA} are the surface excess concentrations of water and

MEA in μmol/m^2. Linearly fitting $\left(\frac{\partial \eta}{\partial x}\right)_{T,P}$ and $\left(\frac{\partial ln\ \gamma}{\partial x}\right)$, as shown in Supporting Figure 6 (a) and (b), enables solving of Γ_{MEA,H_2O} for each bulk mole fraction of MEA. Using the area per molecule

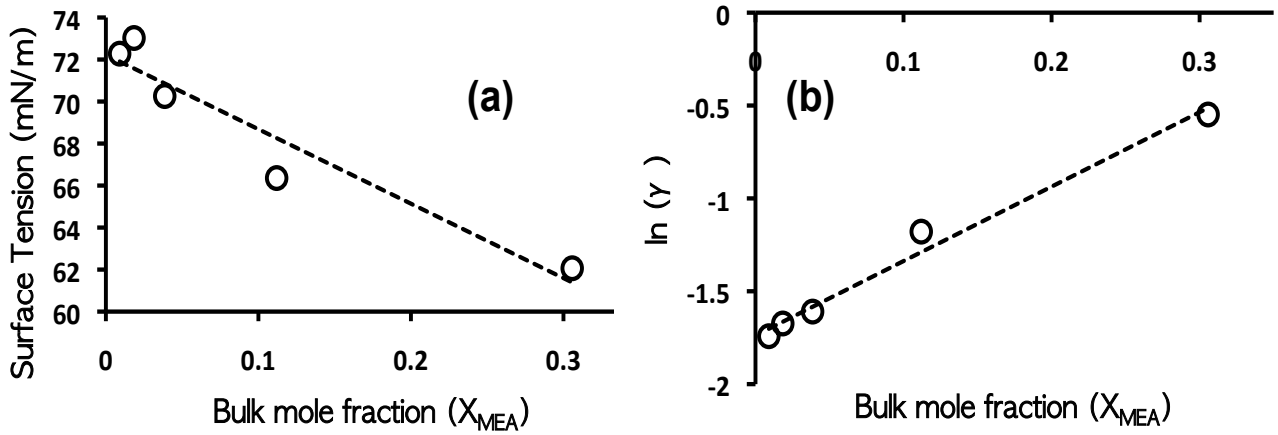

Figure 7: (a) MEA surface tension, η, and (b) the natural log of the activity coefficients, γ, of MEA are plotted as a function of bulk MEA mole fraction. The dashed lines are fits to the data.

(a_i) value of MEA calculated above (126 Å^2) and the known area per molecule value for water (8 Å^2),[3] the relationship of Equation 3 based on the monolayer model may be evoked along with the relationship of surface mole fraction in Equation 4 to solve for surface mole fraction ($m.f._s$) for every bulk mole fraction of MEA.

$$N_{AV}(\Gamma_{H_2O}\ a_{H_2O}\ + \Gamma_{MEA}\ a_{MEA}) = 10^{26} \tag{3}$$

$$m.f._s = \frac{\Gamma_{MEA}}{\Gamma_{MEA} + \Gamma_{H_2O}} \tag{4}$$

Average molecular tilt

Analysis of methylene group average molecular tilt has been extensively studied,[4,6–8] and thus only a brief description of the analysis pertinent to the MEA system is included here.

$$\chi_{ssp}, SS(\theta) = 2\ cos(\theta) \tag{5}$$

$$\chi_{ssp}, AS(\theta) = |-2.106[cos(\theta) - cos^3(\theta)| \quad (6)$$

The results of this analysis for the 10 M MEA spectra are included in Supporting Table 1, where "A" refers to the fitted amplitudes of the peaks. Following the outline of methylene selection rules by Lu, et al., a relationship between the components of $\chi^{(2)}$ and the vibrationally active components of $\beta^{(2)}$ may be made via the orientation of the methylene group. For *ssp*–polarization these relations simplify to Equations 5 and 6, assuming standard methylene bond angles of 109.5° and C_{2v} symmetry.

Table 2: Parameters used for calculating the average molecular tilt for the methylene groups of MEA. Errors calculated from standard deviation of the fitted amplitudes.

	peak 1	peak 2	peak 3	peak 4	A(SS)	A(AS)	A(SS)/A(AS)	$\theta°$
ssp 10M bulk MEA	2845	2873	2920	2936	3.21	1.76	1.82	46±6
ssp 5M bulk MEA	2845	2873	2920	2936	2.17	0.95	2.27	41±3
ssp 1M bulk MEA	2845	2873	2920	2936	0.80	0.40	1.97	45±10

References

(1) Rosen, M. J. *Surfactants and interfacial phenomena*; Wiley Online Library, 2004; Vol. 3.

(2) Rao, Y.; Li, X.; Lei, X.; Jockusch, S.; George, M. W.; Turro, N. J.; Eisenthal, K. B. *The Journal of Physical Chemistry C* **2011**, *115*, 12064–12067.

(3) Tyrode, E.; Johnson, C. M.; Baldelli, S.; Leygraf, C.; Rutland, M. W. *The Journal of Physical Chemistry B* **2005**, *109*, 329–341.

(4) Xu, M.; Liu, D.; Allen, H. C. *Environmental Science & Technology* **2006**, *40*, 1566–1572.

(5) Hilliard, M. D. A predictive thermodynamic model for an aqueous blend of potassium carbonate, piperazine, and monoethanolamine for carbon dioxide capture from flue gas. Ph.D. thesis, University of Texas at Austin, 2008.

(6) Hirose, C.; Akamatsu, N.; Domen, K. *The Journal of Chemical Physics* **1992**, *96*, 997–1004.

(7) Hirose, C.; Yamamoto, H.; Akamatsu, N.; Domen, K. *The Journal of Physical Chemistry* **1993**, *97*, 10064–10069.

(8) Lü, R.; Gan, W.; Wu, B.-H.; Chen, H.; Wang, H.-f. *The Journal of Physical Chemistry B* **2004**, *108*, 7297–7306.